

Interface states effect on conduction mechanisms and barrier height homogeneities of Au/n-GaAs Schottky structures in a wide temperature range

H. Toumi^{a,*}, M. A. Benamara^{a,**,◇}, A. Talbi^{a,*} Z. Benamara^{a,**} Y. Massim^{b,†} and F. Y. M. Benamara^{b,‡}

^aApplied Microelectronics Laboratory, University of Sidi Bel Abbès, Algeria.

* (ORCID:0009-0006-2387-0780), ** (ORCID:0009-0003-3890-4734),

◇ (ORCID:0009-0000-4335-5723), ** (ORCID:0009-0001-4023-6697),

◇ e-mail: mekki_2007@yahoo.fr

^bFaculty of Exact Sciences, University of Sidi Bel Abbès, Algeria.

† (ORCID:0009-0003-2410-6184), ‡ (ORCID:0009-0002-4704-9779).

Received 10 August 2024; accepted 1 October 2025

In this paper, a study of interface states N_{ss} effect on the conduction mechanisms and the barrier height homogeneities of Au/n-GaAs Schottky structures, in a large range of temperatures. As demonstrated, the structure with low N_{ss} shows that the ideality factor n decreases and the barrier height ϕ_b increases as the temperature increases. On the other hand, the structure with high N_{ss} shows that the ideality factor n decreases then increases with increasing temperature. The increasing of the ideality factor in high temperatures is due to the tunnel current, caused by the interface states. The structure of low N_{ss} shows that the dominant current is the TFE conduction mechanism and gives a homogeneous barrier height over all temperature range. While the structure of high N_{ss} shows that the dominant current is TFE at low temperatures (75-300 K) and deviates to FE at high temperatures (300-400 K), and gives an inhomogeneous barrier height.

Keywords: Au/n-GaAs; interface states; electrical behavior; conduction mechanisms; barrier height inhomogeneities; temperature.

DOI: <https://doi.org/10.31349/RevMexFis.72.021001>

1. Introduction

GaAs semiconductor has attracted intense interest in the past few years. This is due to its properties such as wide bandgap, high break down field, higher mobility, and thermal stability [1-3]. Also, GaAs is widely used in various applications such as microwave field-effect transistors, light-emitting diodes, high-temperature electronics, high-density optical data storage devices, solar cells and atmospheric remote sensing devices [4-6]. However, the efficiency and the accuracy of these structures are drastically related to the interface quality [5,7,8]. The interface states behave like recombination-generation centers that affect the conduction mechanism and electrical behavior of the device [3]. In this paper, we use Silvaco-Atlas software to perform a detailed simulation study of the interface states effect on the electrical parameters of Au/n-GaAs Schottky structure [9].

2. Simulation part

Silvaco-Atlas software is used to study the effect of the interface states density N_{ss} on the electrical behavior of Au/n-GaAs Schottky contact. In simulating the transport of carriers across a three-dimensional grid, Silvaco-Atlas predicts the electrical characteristics of the structure [9]. Many parameters should be identified such as mesh, regions, electrode positions, doping density, and interface states density.

Once specified, all electrical and optical properties are considered by Atlas: band gap E_g , states densities N_c, N_v , electron affinity χ , mobilities μ_n, μ_p , and dielectric constant

ϵ . Models used include SRH, Auger, CONMOB, Incomplete, and FLDMOB [9].

$$N_{ss} = g_{TA}(E) + g_{TD}(E) + g_{GA}(E) + g_{GD}(E), \quad (1)$$

$$g_{TA}(E) = N_{TA} \exp\left(\frac{E - E_c}{W_{TA}}\right), \quad (2)$$

$$g_{TD}(E) = N_{TD} \exp\left(\frac{E_v - E}{W_{TD}}\right). \quad (3)$$

The two structures simulated are:

- Low interface density: $N_{ss} = 1 \times 10^{10} \text{ cm}^{-2} \text{ eV}^{-1}$
- High interface density: $N_{ss} = 5 \times 10^{12} \text{ cm}^{-2} \text{ eV}^{-1}$

3. Simulation results

Figures 1 and 2 show the semi-logarithmic current-voltage (I-V) curves for the two densities.

From Fig. 1, the structure with low N_{ss} shows typical Schottky behavior, with decreasing current as temperature decreases, in agreement with experimental results [10-13]. In Fig. 2, deviation from linearity is visible at low bias, more pronounced at high temperature.

$$I = I_s \left[\exp\left(\frac{q(V - IR_s)}{nkT}\right) - 1 \right], \quad (4)$$

$$I_s = AA^* T^2 \exp\left(-\frac{q\phi_b}{kT}\right). \quad (5)$$

Table I lists the series resistance values R_s for both structures at different temperatures.

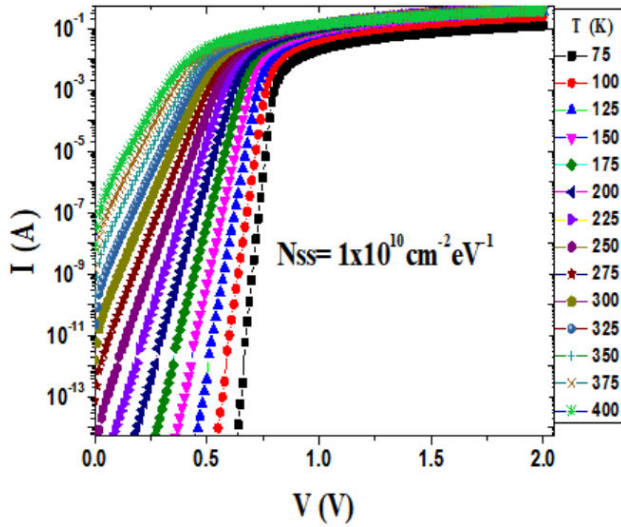


FIGURE 1. I-V characteristics for low interface states density ($N_{ss} = 1 \times 10^{10}$).

TABLE I. Series resistance (R_s) values of the two structures for different temperatures.

T (K)	$N_{ss} = 1 \times 10^{10}$		$N_{ss} = 5 \times 10^{12}$	
	R(G-I)	R(H-I)	R(G-I)	R(H-I)
75	9.58	9.47	9.56	9.44
100	4.72	4.67	4.72	4.66
125	3.33	3.30	3.33	3.29
150	2.83	2.80	2.83	2.79
175	2.66	2.63	2.66	2.63
200	2.64	2.62	2.64	2.61
225	2.72	2.69	2.72	2.69
250	2.84	2.82	2.85	2.82
275	3.00	2.98	3.00	2.97
300	3.18	3.16	3.18	3.15
325	3.38	3.35	3.36	3.32
350	3.58	3.55	3.54	3.50
375	3.80	3.76	3.76	3.73
400	4.00	3.98	4.00	4.00

As it can be seen, the interface states with $N_{ss} = 5 \times 10^{12}$ have no effect on the series resistance compared to the structure with $N_{ss} = 1 \times 10^{10}$ over all temperature range.

The structure with low N_{ss} (Fig. 3) shows that n decreases and ϕ_b increases as the temperature increases. It can be seen that n and ϕ_b vary from 1.43 and 0.64 eV at 75 K to 1.10 and 0.77 eV at 400 K, respectively. These results are in accordance with the reported experimental studies [10-12].

On the other hand, the structure with high N_{ss} (Fig. 4) shows that n decreases from 1.69 at 75 K to 1.17 at 275 K, then, contrary to the structure of low N_{ss} , it increases to 1.73 at 400 K. The increase of the ideality factor at high temperatures is attributed to the influence of tunnel currents such as thermionic field emission (TFE) and field emission (FE)

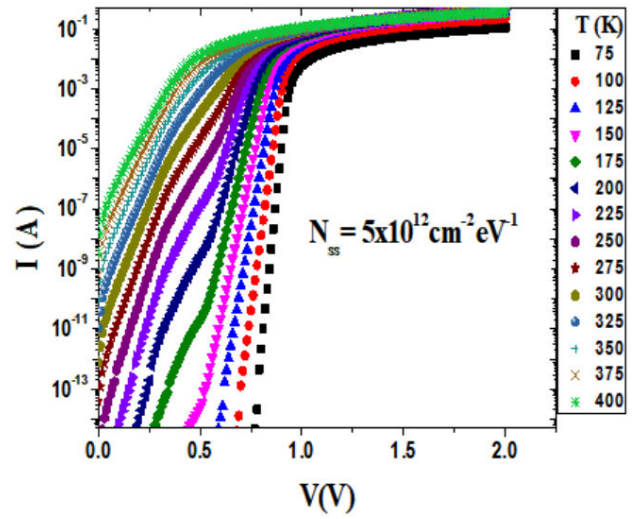


FIGURE 2. I-V characteristics for high interface states density ($N_{ss} = 5 \times 10^{12}$).

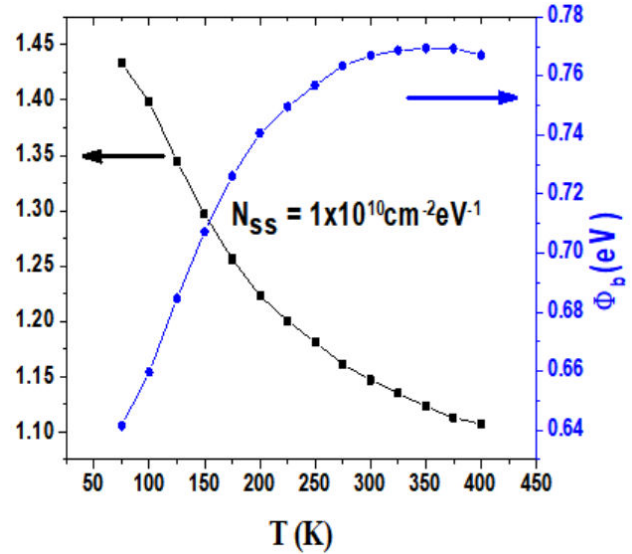


FIGURE 3. Temperature dependence of n and ϕ_b of the structure with low interface states density ($N_{ss} = 1 \times 10^{10} \text{ cm}^{-2} \text{ eV}^{-1}$).

mechanisms [10,20]. Similarly, ϕ_b increases from 0.64 eV at 75 K to 0.89 eV at 275 K, then decreases to 0.67 eV at 400 K. These results indicate that the interface states have an influence on the ideality factor and the barrier height, with an important effect at high temperatures.

The tunneling current is given by [15,19-22]:

$$I = I_{\text{tun}} \left[\exp \left(\frac{q(V - IR_s)}{E_0} \right) - 1 \right], \quad (6)$$

$$\frac{E_0}{kT} = \frac{E_{00}}{kT} \coth \left(\frac{E_{00}}{kT} \right), \quad (7)$$

$$E_{00} = \frac{h}{4\pi} \left(\frac{N_D}{m_e^* \epsilon_s} \right)^{1/2}, \quad (8)$$

where E_{00} the characteristic tunneling energy, h the Planck constant, E_0 is independent of temperature and equal to E_{00} .

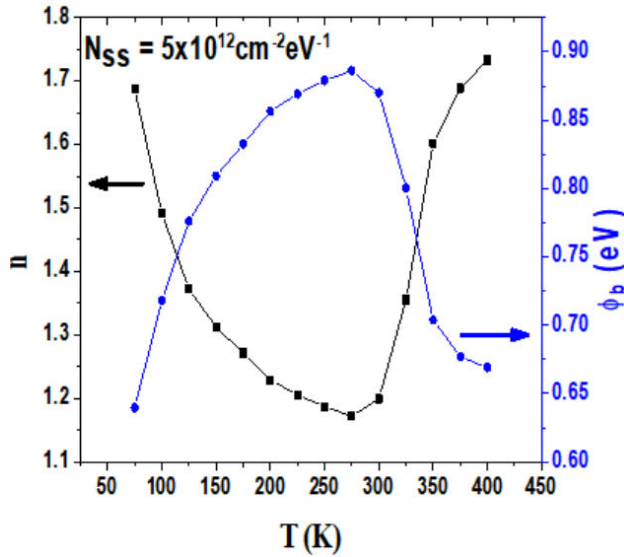


FIGURE 4. Temperature dependence of n and ϕ_b of the structure with high interface states density ($N_{ss} = 5 \times 10^{12} \text{ cm}^{-2} \text{ eV}^{-1}$).

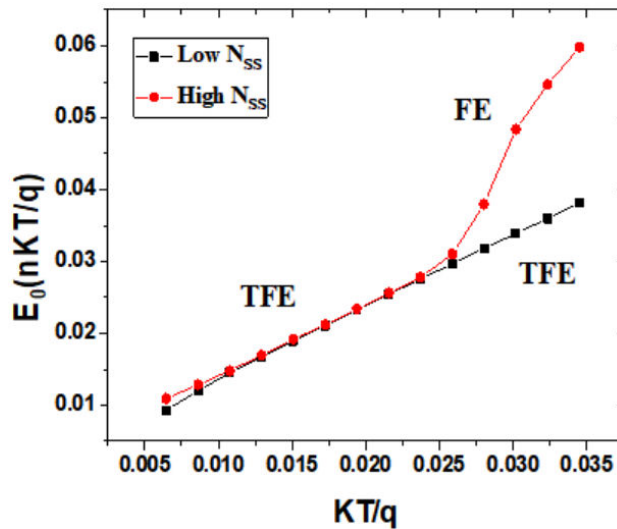


FIGURE 5. Variation of nkT/q vs kT/q for structures with low and high interface states density.

Figure 5 illustrates $E_0(nkT/q)$ versus kT/q plots of the structures for low and high interface state densities.

Figure 5 shows that for the structure with low N_{ss} , E_{00} is approximately equal to kT/q for all temperatures. This means that the thermionic field emission (TFE) conduction mechanism across all temperature ranges is the dominant current [10]. While, the structure with high N_{ss} shows that the dominating current at low temperatures (75 – 300 K) is the TFE mechanism, then the field emission (FE) mechanism becomes dominant at high temperatures (300 – 400 K), where $E_{00} \gg kT/q$, which is due to the interface states effect.

These results explain the increase of the ideality factor at high temperatures and the deviation from linearity of the current-voltage characteristics at low voltages for the structure with high interface states density (Fig. 2). It is also

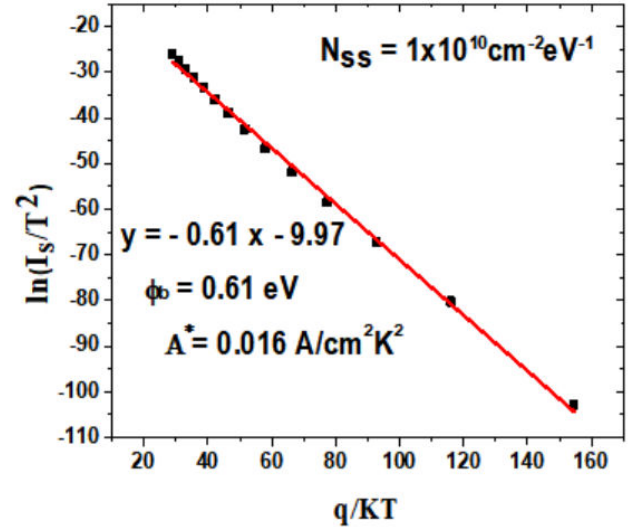


FIGURE 6. $\ln(I_s/T^2)$ versus q/kT for the structure with low interface states density ($N_{ss} = 1 \times 10^{10} \text{ cm}^{-2} \text{ eV}^{-1}$).

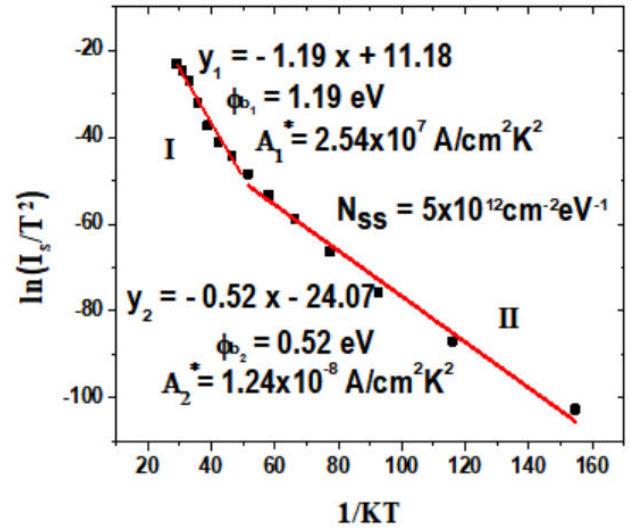


FIGURE 7. $\ln(I_s/T^2)$ versus q/kT for the structure with high interface states density ($N_{ss} = 5 \times 10^{12} \text{ cm}^{-2} \text{ eV}^{-1}$).

also clearly observed that interface states with $N_{ss} = 5 \times 10^{12} \text{ cm}^{-2} \text{ eV}^{-1}$ have no considerable effect on the conduction mechanisms at low temperatures.

To study the effect of the interface states on the inhomogeneities of the barrier height, Figs. 6 and 7 show the Richardson plots $\ln(I_s/T^2)$ versus q/kT for structures with low and high interface states density, respectively. Where, the relation is given by:

$$\ln\left(\frac{I_s}{T^2}\right) = \ln(AA^*) - \frac{q\phi_b}{kT}. \quad (9)$$

Figure 6 presents a linear curve of the Richardson characteristics, which is attributed to the homogeneity of the barrier height for low N_{ss} [14], where ϕ_b and A^* are estimated to 0.61 eV and $0.016 \text{ A cm}^{-2} \text{ K}^{-2}$, respectively.

As depicted in Fig. 7, the structure with high N_{ss} shows two linear behaviors of the Richardson characteristics, which

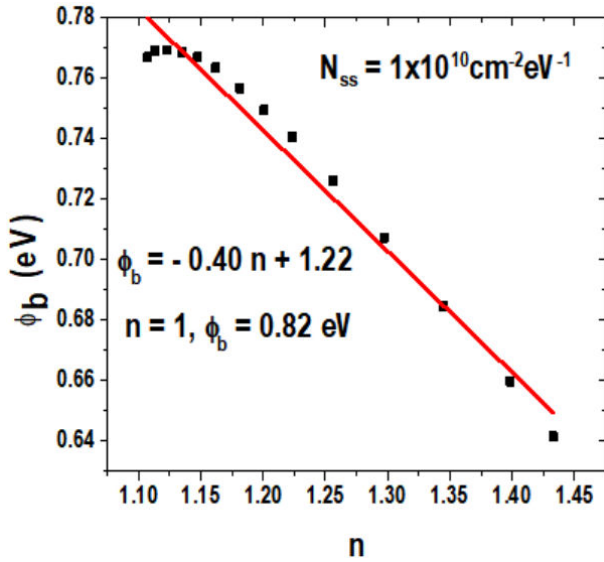


FIGURE 8. Plot of ϕ_b vs n of Au/n-GaAs structure with low interface states density ($N_{ss} = 1 \times 10^{10} \text{ cm}^{-2} \text{ eV}^{-1}$).

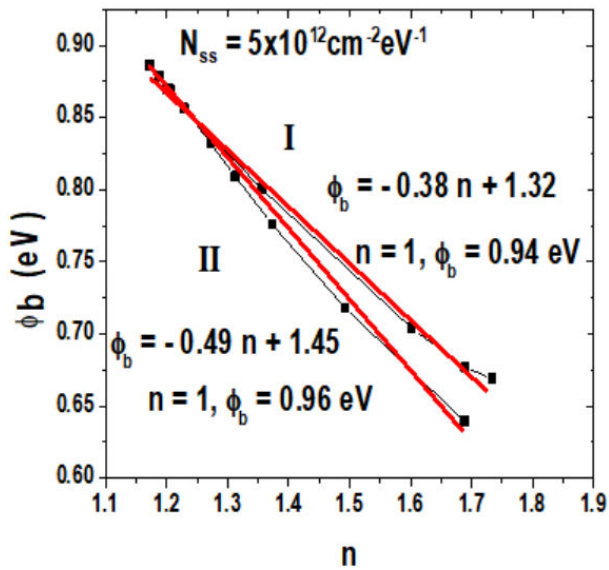


FIGURE 9. Plot of ϕ_b vs n for high interface states density ($N_{ss} = 5 \times 10^{12} \text{ cm}^{-2} \text{ eV}^{-1}$).

corresponds to the inhomogeneous barrier height of the structure; where ϕ_b and A^* are estimated to 1.19 eV and $2.54 \times$

$10^7 \text{ A cm}^{-2} \text{ K}^{-2}$, respectively, in region I, and to 0.52 eV and $1.24 \times 10^{-8} \text{ A cm}^{-2} \text{ K}^{-2}$, respectively, in region II.

Werner and Güttler [23] suggested that the different values of ϕ_b correspond to the fluctuation of the barrier height as a Gaussian distribution. The A^* obtained for both structures is very far from the theoretical value, which is equal to $8.16 \text{ A cm}^{-2} \text{ K}^{-2}$ for n-GaAs.

Figures 8 and 9 give the characteristics of ϕ_b versus n of Au/n-GaAs Schottky structures with low and high interface states density, respectively.

4. Discussion and conclusion

As shown in Fig. 8, Au/n-GaAs structure with low N_{ss} gives a linear curve that is attributed to the homogeneities of the barrier height, where the value of ϕ_b for $n = 1$ is estimated to 0.82 eV. Figure 9 shows that the structure with high N_{ss} presents two linear curves, which are attributed to the inhomogeneity of the barrier height [24,25], where ϕ_b for $n = 1$ is equal to 0.94 eV in region I and equal to 0.96 eV in region II.

These results confirm the above results obtained from the Richardson's properties and indicate clearly the effect that the interface states cause due to the inhomogeneity of the barrier height of the Schottky structures.

Conclusion

A study of interface states effect on Au/n-GaAs Schottky structures is investigated. The structure with low N_{ss} shows that n decreases and ϕ_b increases as the temperature increases, where the values of n and ϕ_b range from 1.43 and 0.64 eV at 75 K to 1.1 and 0.77 eV at 400 K, respectively. On the other hand, the structure with high N_{ss} shows that n decreases from 1.69 at 75 K to 1.17 at 275 K, then increases to 1.73 at 400 K with increasing temperature.

The increasing of the ideality factor at high temperatures is due to the tunnel current caused by the interface states. The dominant current in the structure of low N_{ss} is the TFE conduction mechanism over all temperature range. While, the dominant current in the structure of high N_{ss} is TFE at low temperatures (75-300 K) and deviates to FE at high temperatures (300-400 K) due to the interface states effect. The structure of low N_{ss} exhibits a homogeneous barrier height, while the structure of high N_{ss} shows an inhomogeneous barrier height.

1. T. Hariu, N. Suzuki, K. Matsushita, and Y. Shibata, "Nitride-based passivation of GaAs for reduced surface state density," in *1978 International Electron Devices Meeting*, 1978, pp. 598-599.
2. H.-H. Lu, J.-P. Xu, L. Liu, P.-T. Lai, and W.-M. Tang, "Electrical and interfacial properties of GaAs MOS capacitors with

La-doped ZrON as interfacial passivation layer," *IEEE Transactions on Electron Devices*, **64** (2017) 2179.

3. M. A. Ebeoğlu, "Current-voltage characteristics of Au/GaN/GaAs structure," *Physica B: Condensed Matter*, **403** (2008) 61.
4. A. Rabehi, M. Amrani, Z. Benamara, B. Akkal, and A. Kacha,

- “Electrical and photoelectrical characteristics of Au/GaN/GaAs Schottky diode,” *Optik*, **127** (2016) 6412.
5. R. Schmitsdorf, T. Kampen, and W. Mönch, “Correlation between barrier height and interface structure of AgSi (111) Schottky diodes,” *Surface Science*, **324** (1995) 249.
 6. M. Soyulu and F. Yakuphanoglu, “Analysis of barrier height inhomogeneity in Au/n-GaAs Schottky barrier diodes by Tung model,” *Journal of Alloys and Compounds*, **506** (2010) 418.
 7. N. Paul, Y. Ohta, D. Tezuka, M. Nasuno, Y. Yamamura, T. Inokuma, K. Iiyama, and S. Takamiya, “Quality improvement of oxidized-GaAs/n-GaAs structure by nitrogen plasma treatment,” in *Conference Proceedings. 14th Indium Phosphide and Related Materials Conference (Cat. No. 02CH37307)*, (2002), pp. 217-220.
 8. Z. J. Horváth *et al.*, “Effect of interface roughness and morphology on the electrical behaviour of Au/n-GaAs Schottky diodes,” in *ASDAM 2000. Conference Proceedings. Third International EuroConference on Advanced Semiconductor Devices and Microsystems (Cat. No. 00EX386)*, (2000), pp. 257-259.
 9. S. Int, “ATLAS user’s manual a 2D numerical device simulator, 2004,” ed, (2016).
 10. E. Özavcı, S. Demirezen, U. Aydemir, and Ş. Altındal, “A detailed study on current-voltage characteristics of Au/n-GaAs in wide temperature range,” *Sensors and Actuators A: Physical*, **194** (2013) 259.
 11. M. Hudait, P. Venkateswarlu, and S. Krupanidhi, “Electrical transport characteristics of Au/n-GaAs Schottky diodes on n-Ge at low temperatures,” *Solid-State Electronics*, **45** (2001) 133.
 12. S. Hardikar, M. Hudait, P. Modak, S. Krupanidhi, and N. Padha, “Anomalous current transport in Au/low-doped n-GaAs Schottky barrier diodes at low temperatures,” *Applied Physics A*, **68** (1999) 49.
 13. D. Korucu, A. Turut, and H. Efeoglu, “Temperature dependent I-V characteristics of an Au/n-GaAs Schottky diode analyzed using Tung’s model,” *Physica B: Condensed Matter*, **414** (2013) 35.
 14. H. Helal, Z. Benamara, M. B. Arbia, A. Khetrou, A. Rabehi, A. H. Kacha, and M. Amrani, “A study of current-voltage and capacitance-voltage characteristics of Au/n-GaAs and Au/GaN/n-GaAs Schottky diodes in wide temperature range,” *International Journal of Numerical Modelling: Electronic Networks, Devices and Fields*, p. e2714.
 15. Ş. Karataş *et al.*, “Temperature dependence of barrier heights of Au/n-type GaAs Schottky diodes,” *Solid-State Electronics*, **49** (2005) 1052.
 16. E. Rhoderick and R. Williams, *Metal-Semiconductor Contacts*, (Clarendon Press, Oxford, 1988).
 17. M. Biber, C. Coşkun, and A. Türit, “Current-voltage-temperature analysis of inhomogeneous Au/n-GaAs Schottky contacts,” *The European Physical Journal Applied Physics*, **31** 2005 79.
 18. H. Helal *et al.*, “Comparative study of ionic bombardment and heat treatment on the electrical behavior of Au/GaN/n-GaAs Schottky diodes,” *Superlattices and Microstructures*, **201** (2019) 9276.
 19. S. Cheung and N. Cheung, “Extraction of Schottky diode parameters from forward current-voltage characteristics,” *Applied Physics Letters*, **49** (1986) 85.
 20. M. Çavas, F. Yakuphanoglu, and Ş. Karataş, “The electrical properties of photodiodes based on nanostructure gallium doped cadmium oxide/p-type silicon junctions,” *Indian J Phys*, **91** (2017) 413.
 21. F. Padovani and G. Sumner, “Experimental Study of Gold-Gallium Arsenide Schottky Barriers,” *Journal of Applied Physics*, **36** (1965) 3744.
 22. F. Padovani, “Graphical determination of the barrier height and excess temperature of a Schottky barrier,” *Journal of Applied Physics*, **37** (1966) 921.
 23. J. H. Werner and H. H. Güttler, “Barrier inhomogeneities at Schottky contacts,” *Journal of Applied Physics*, **69** (1991) 1522.
 24. R. Schmitsdorf, T. Kampen, and W. Mönch, “Correlation between barrier height and interface structure of AgSi (111) Schottky diodes,” *Surface Science*, **324** (1995) 249.
 25. M. Soyulu and F. Yakuphanoglu, “Analysis of barrier height inhomogeneity in Au/n-GaAs Schottky barrier diodes by Tung model,” *Journal of Alloys and Compounds*, **506** (2010) 418.